Journal of Mechanical Research and Application,
Vol. 2, No. 1, 2010, 55-61

JMRA

Hydrodynamic Performance of the Modern Ship Propulsion System

Hassan Ghassemi[1*], Roya Shademani[2]

Received: 24 May 2009; Accepted: 29 September 2009

Abstract: This paper presents numerical calculations for podded propulsion system using vortex theory and potential panel method. The method discretizes the surface boundary of the body (propeller +pod+strut) and obtained the vortex and propeller surface and potential on strut and pod. A model propeller and strut are considered for these calculations and the results of pressure distribution, flow field around the propeller and hydrodynamic characteristics of the propeller are given. The calculated hydrodynamic characteristics of the propeller are compared with the experimental data and it is shown in good agreement with them.

Keywords: Hydrodynamic Characteristics, Podded Propulsion, Panel Method

1. Introduction

The conventional propellers are mounted on a shaft and the upstream wake consists of a non-uniform velocity so causes cavitation and vibrations that can affect the hull. Because of the recent major improvements made by engine manufacturers in electrical propulsion, in terms of power levels and compactness, it is now possible to envisage ships equipped with electrical propellers suspended in pods. This concept has the obvious hydrodynamic advantage of making it possible to control the pod's trim and drift angle so that the propeller is set in a regular flow. This new configuration also removes the need for the drive shaft and the propeller brackets, which causes a disturbance in the regularity of the wake and results in a considerable increase in the total resistance to motion [1]

Because of importance the hydrodynamic characteristics of inflow velocity, we can use podded drives. Therefore the propeller works in the homogenous water inflow so wake field into the propeller will be homogeneous, as there are no appendages in front of the propeller. For steering the vessel, it is used by small rudder at the rear of the vertical hydrofoil (stem), like a flap on an aircraft wing. Such a system has the following qualities [2]:

- Reduced machinery space
- Excellent maneuverability
- Sufficient immersion with high efficiency even in heavy seas
- Homogenous inflow gives ideal conditions for avoidance of cavitation which gives reduction in propeller efficiency and risk of blade erosion
- Improved thrust/torque ratio and thereby total efficiency due to the interaction between propeller and podded unit.
- Sufficient clearance between propeller and hull.

The first author started the research on various marine propellers since 15 years ago and prepared his own code, namely SPD (ship propulsor design). This code is based on potential boundary element method including boundary layer theory for viscous effect. CRP is a system for energy saving and may be useful for some ships especially for torpedo and submarines. This paper is a small part of the results for the hydrodynamics characteristics (open water) of propeller alone and CRP system are presented.

The numerical results are obtained for the propeller, strut and pod. Hydrodynamic propeller characteristics are compared and the results are shown in good agreement with the experimental one. Pressure distribution on strut and pod, flow field around the strut are also given.

$$2\pi\phi_P = \int_{S_B}\left\{\phi(q)\frac{\partial}{\partial n_q}\left(\frac{1}{R}\right) - \frac{\partial\phi(q)}{\partial n_q}\left(\frac{1}{R}\right)\right\}dS_B + \int_{S_W}\left\{\Delta\phi(q)\frac{\partial}{\partial n_q}\left(\frac{1}{R}\right) - \Delta\frac{\partial\phi(q)}{\partial n_q}\left(\frac{1}{R}\right)\right\}dS_W \quad (1)$$

1*. Corresponding Author: Associate Professor, Faculty of Marine Technology, Amirkabir University of Technology, Tehran, Iran (gasemi@cic.aut.ac.ir)
2. PhD. Student, Faculty of Marine Technology, Amirkabir University of Technology, Tehran, Iran (shademan@cic.aut.ac.ir)

2. Mathematical formulation

2.1. Vortex and potential on the propeller

The propeller is rotating with a constant angular velocity ω around the $x-$axis. The propeller is represented hydrodynamically by the vortex system, i.e. the bound vortex arranged $\Gamma(r,\vartheta)$ in the radial direction on S_P and the free vortex $h(r)$ shedding from the bound vortex. And it is distributed on the helical surface with the pitch $2\pi h(r)$ without contraction. The velocity potential ϕ_P due to the bound vortex on the propeller may be expressed as:

$$\phi_P = \int_{r_B}^{r_0} r' dr' \int_0^{2\pi} \Gamma(r',\vartheta') G_P(x,r,\vartheta;r',\vartheta') d\vartheta' \tag{2}$$

Where:

$$G_P(x,r,\vartheta;r',\vartheta') = \frac{r'}{h(r')}\frac{1}{R_P} + \frac{-r\cos\vartheta\sin\vartheta' + r\sin\vartheta\cos\vartheta'}{{R_P}^2 - x^2}\left(1+\frac{x}{R_P}\right) \tag{3}$$

The propeller is considered to have the finite number of blades and finite chord length, bound and free vortices are determined from the kinematics boundary condition (KBC) [3].

2.2. Potential on strut- flap- pod (SFP)

The coordinate system for podded propulsion system is shown in Fig. 1. It is defined a rectangular coordinate system $O-XYZ$ and a cylindrical system $O-Xr\theta$ fixed in space. The origin is located at the center of the propeller and the $x-$axis coincides with the propeller shaft axis. The steering pod is placed behind the propeller and is parallel to the $z-$axis.

As usual, the fluid is assumed to be inviscid, incompressible and irrotational. The totapotential Φ is summation of the perturbation velocity potential ϕ and given inflow velocity $\vec{V}_I$ as follows:

$$\Phi = \vec{V}_I x + \phi \tag{4}$$

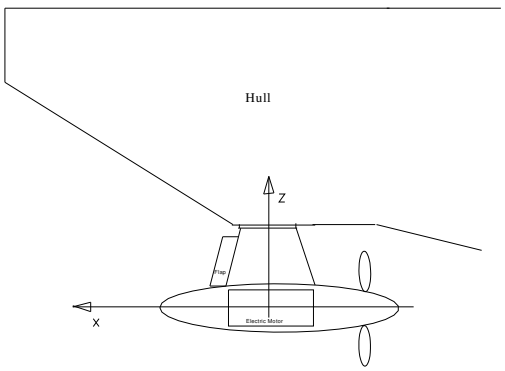

Fig. 1. Coordinate System for Podded Propulsion System

A perturbation velocity potential, φ, represents the flow field around a body, which satisfies the Laplace's equation:

$$\nabla^2\phi = 0 \tag{5}$$

and vanishes at infinity. We consider a closed domain boundary surface S, which is composed of body and wake. Applying Green's theorem, perturbation velocity potential at any field point $P(x,y,z)$` can be expressed by a distribution of source and doublet over the boundary surface S_B.

Where:

ϕ_P	Perturbation velocity potential
$p(x,y,z)$	Field point where induced potential is calculated
$q(\zeta,\eta,\xi)$	Singularity point where is located
$\frac{\partial}{\partial n}$	Normal derivative with respect to the point q
R	distance between p and q

This equation may be regarded as a representation of the velocity potential in terms of a normal dipole distribution of strength ϕ_P on the body surface $p(x,y,z)$, a source distribution of strength $\frac{\partial\phi}{\partial n}$ on S_B, and a normal dipole distribution of strength $\Delta\phi$ on the wake surface S_W [4].

3. Numerical results and discussion

3.1. Propeller and SFP models

In order to evaluate the accuracy and applicability of the method, a typical propeller (MP195) plus SFP011.

Models have been selected principal particulars of the propeller models are shown in tables 1 and 2. Panel arrangement on podded propulsion system is shown in Fig. 2.

Table 1. Principal particulars of propeller models

Propeller Type	MP195
Diameter [mm]	250
Exp. Area Ratio	0.65
Pitch Ratio	0.710
Boss Ratio	0.18
No. of Blades	5
Rake Angle [Deg.]	10.0
Max. Blade Width Ratio	0.249
Max. Blade Thickness Ratio	0.050
Blade Section	MAU

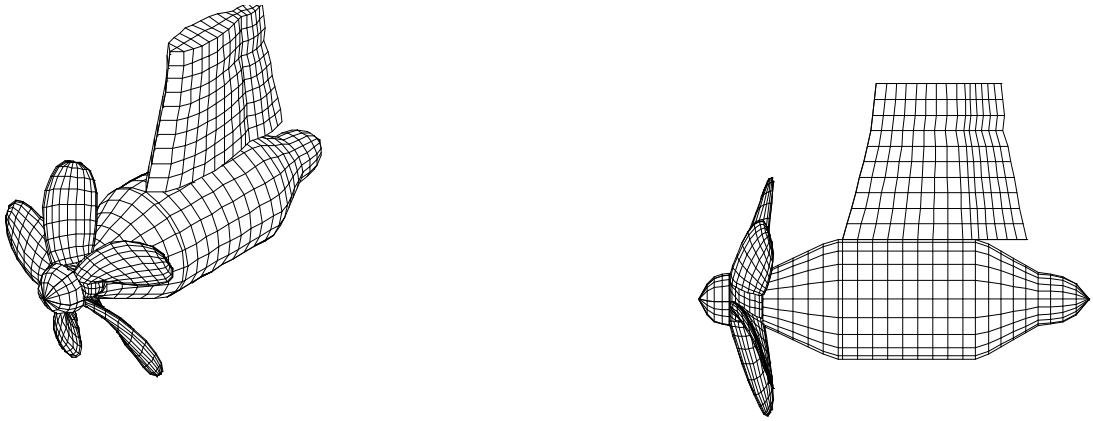

Fig. 2. Panel arrangement on podded propulsion system

Table 2. Principal particulars of SFP

Strut-Flap-Pod	SFP011
Mean Chord Length (mm)	121
Flap-Strut Ratio	0.35
Span (mm)	142
Mean Thickness (mm)	16.5
Length between Propeller and Strut (mm)	150
Type of Section	Normal
Pod Diameter (mm)	100

3.2. Velocity field behind the propeller

Computations were performed for the podded propulsion system at different operating conditions. After calculating the vortex and potential from kinematic boundary condition, a postprocessor was used to compute the velocity components for grid points in a transverse plane down position of the propeller plane. The velocity field behind the propeller is important from the point of view of inflow velocity to strut/flap and pod. so induced velocities acted by propeller to the SFP and vise-versa measure mutual interaction between the propeller and SFP. Giving the inflow velocity $\vec{V}_I$, the velocity components $\vec{V}_P$ flowing towards the propeller is expressed as:

$$\vec{V}_P = \vec{V}_I + \nabla\phi_{SFP} \tag{6}$$

and the velocity components $\vec{V}_{SFP}$ flowing onto the SFP is expressed as:

$$\vec{V}_{SFP} = \vec{V}_I + \vec{w}_P + \nabla\phi_P \tag{7}$$

here $\vec{W}_P$ is non-potential flow velocity. $\nabla\phi_P$ and $\nabla\phi_{SFP}$ are induced velocities by propeller and SFP, respectively. An interactive process is required till all propulsion coefficients lead to converged. On the other hand, the induced velocity generated by SFP acting to the propeller has not been affected.

The computed results for the 2-D cross velocity are given in Figs. 3 and 4 at different advance ratios and downstream positions. the velocity on strut/flap in propeller slipstream at different operating condition on both sides (pressure and suction) are shown.

3.3. Pressure distribution on SFP

To integrate force and torque we need the pressure on each panel. The pressure follows Bernoulli's equation:

$$p - p_0 = -\frac{1}{2}\rho\left[V_I^2 - \left(\vec{V}_I - \left(\vec{V}_I \cdot \vec{n}\right)\vec{n} + \nabla\phi\right)^2\right] \tag{8}$$

The surface pressure distribution is one of the most essential step to understand the capability of the potential panel method. It is well known that any rough panel division of the surface will affect the results of pressure distribution. Then it needs to have fairer surface with high precision interpolation for the coordinates of the body. The connection between the strut and flap is an important point when it turns. A flap deflection down causes a suction peak at the right side near the flap hinge. Fig. 5 shows calculated pressure distribution along a strut/flap profile at inflow angle 0 degrees and flap angle 10 degrees.

3.4. Hydrodynamic characteristics of the podded propulsion system

Pressure distribution along the pod is shown in Fig. 6 at $J = 0.458$ when the strut/flap is located above it. The bigger negative pressure can be seen where the flap is located with some angle. The non-regularity pressure is obtained at the nose of pod so this maybe due to propeller disturbance.

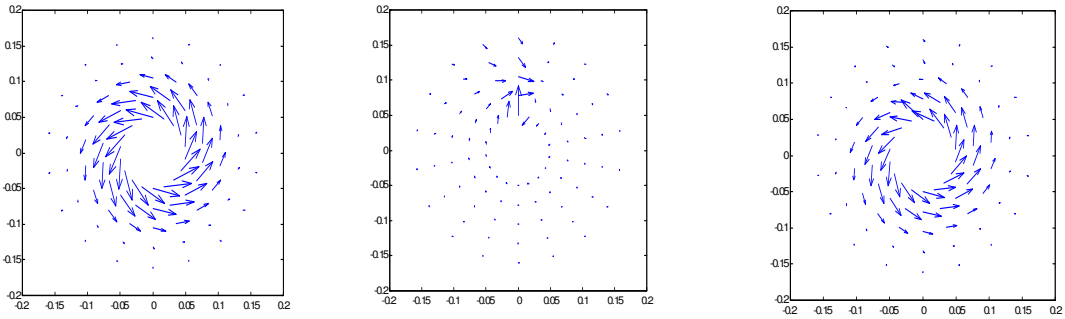

Fig. 3. Induced velocity contour behind the propeller (J=0.458, flap ang.=10deg., x/D=0.8)

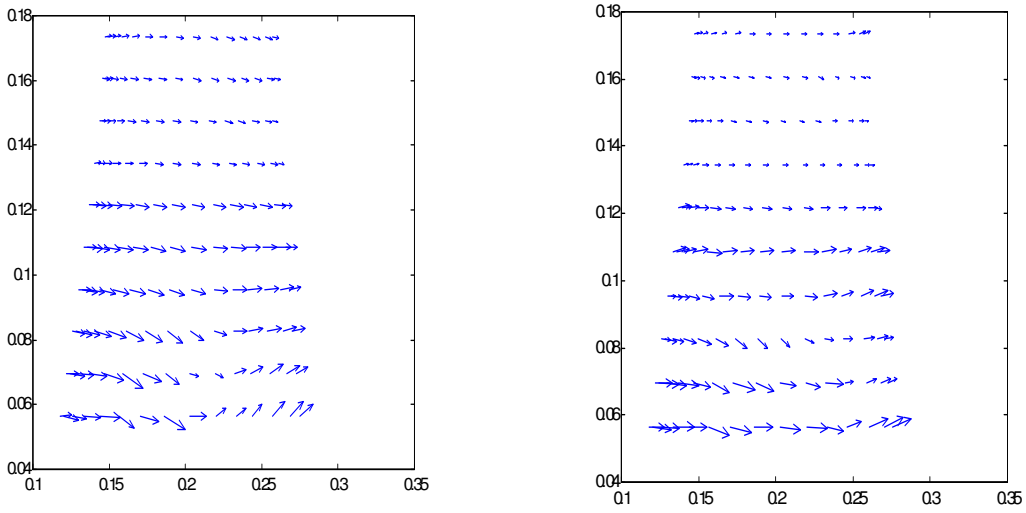

Fig. 4. Velocity on strut/flap in propeller slipstream (J=0.458, flap ang.=10deg.)

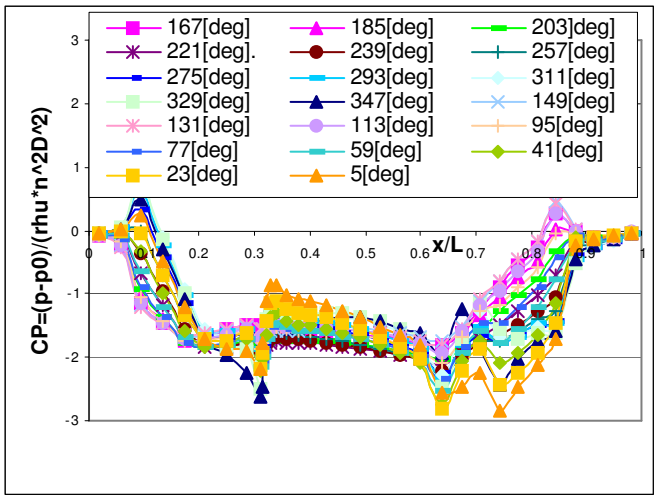

Fig. 5. Pressure distribution along pod (J=0.458)

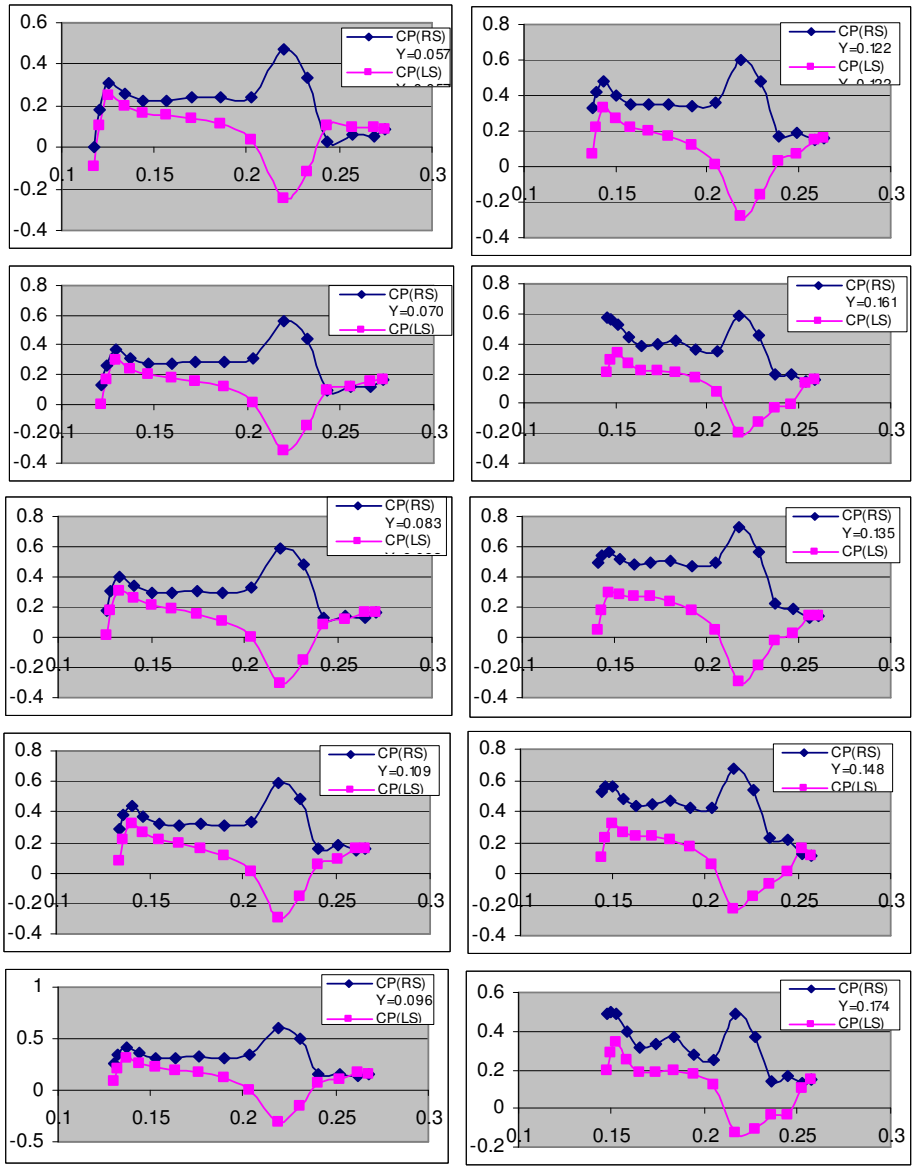

Fig. 6. Pressure distribution on strut/flap behind the propeller (J=0.458, Flap ang.=10deg.)

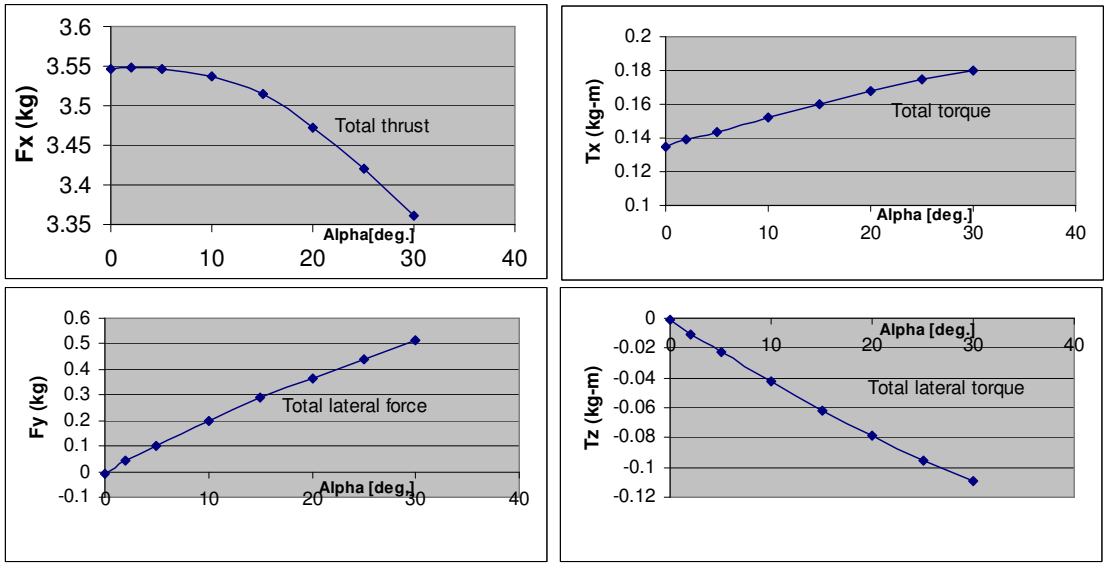

Fig. 7. Calculated hydrodynamic forces of podded propulsion System (MP195, J=0.458)

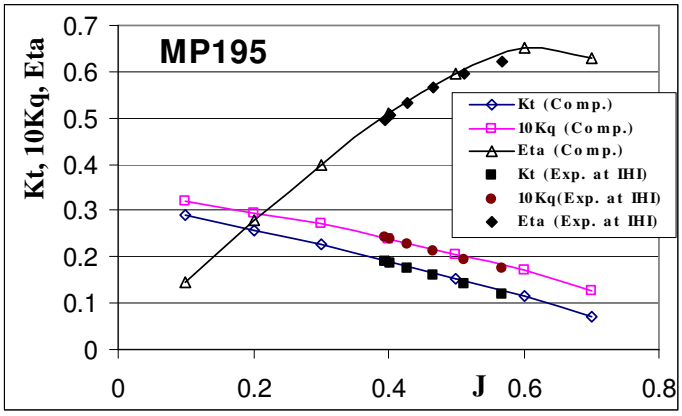

Fig. 8. Comparison of Propeller Characteristics of MP195

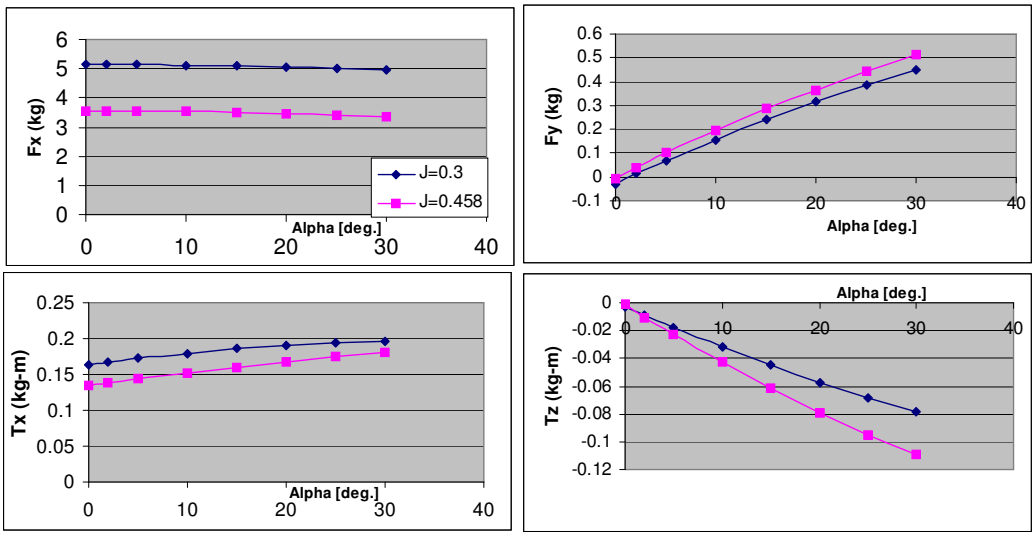

Fig. 9. Calculated hydrodynamic force and torque of podded propulsion system at different advance ratio

A comparison with corresponding experimental studies for MP195 propeller performance in open water condition is shown in Fig. 8. The computed open water characteristics of MP195 are confirmed to be in good agreement with experimental data. The hydrodynamic coefficients (Kt, Kq and η are thrust, torque and efficiency, respectively) are expressed:

$$J=\frac{V_A}{nD};K_t=\frac{F_X}{\rho n^2D^4};K_q=\frac{T_X}{\rho n^2D^5};\eta=\frac{J}{2\pi}\cdot\frac{K_t}{K_q} \tag{9}$$

Where J is advance coefficient and F_X, F_Y and T_X are forces and torque. Sometimes T_Z in high angle is an important parameter, while F_Z and T_Y are very small even in high angles (they are defined according to our $O-XYZ$ coordinate system). Figs. 7 and 9 show the total thrust, lateral forces and torque on MP195+SFP011 at different flap angles. It is clear that when flap angle is increased, it causes the total thrust to decrease while the torque is increased. We cannot judge and discuss further without experimental data, but it is estimated regarding our promising insights and some computational and experimental results for conventional propulsion system, in which they have the same tendency with our calculated results.

4. Conclusions

A computational capability has been developed to predict the local flow field around podded propulsion systems. Inflow to strut/flap and pod is computed by summation of induced velocity and non-potential velocity using propeller theory. The downstream velocity components at different positions have been presented as two-dimensional velocity vectors of cross velocity and contour plots of the axial velocity.

Hydrodynamic forces and torque for MP195 propeller model and SFP011 at different angles have been carried out. Hopefully, those calculated

results would be validated with experimental data in the near future.

Further studies could consider for ducted podded propeller system and its modeling the flow in off-design conditions during maneuvering. The effect of profile thickness of strut/flap and diameter of pod, twin-podded propulsors behind the ship hull and their interactions are interesting points to be investigated more in detail.

References

[1] Achkinadze, A. S.; Berg, A.; Krasilnikov; V. I. and Stepanov, I. E., "Numerical Analysis of Podded and Steering Systems Using a Velocity Based Source Boundary Element Method with Modified Trailing Edge", Proceedings of the Propellers/ Shafting, SNAME, Virginia Beach, VA, USA, 17-18 Sept., 2003.

[2] Stettler, J.W., "Steady and Unsteady Dynamics of an Azimuthing Podded Propulsor Related to Vehicle Maneuvring", PhD Dissertation, Massachusetts Institute of Technology, 2004.

[3] Kinnas, S.; Natarajan, S.; Lee, H.; Kakar, K.; Gupta, A., "Numerical Modelling of Podded Propulsors and Rudder Cavitation", Proceedings of the Propellers/ Shafting, SNAME, Virginia Beach, VA, USA, 17-18 Sept., 2003.

[4] Kerwin, J.; Taylor, T.; Black, S.; Mchugh, G., "A Coupled Lifting-Surface Analysis Technique for Marine Propulsors in Steady Flow", Proceedings of the Propellers/ Shafting'97 Symposium, Virginia Beach, VA, USA, 1997, 20, 1-15.